

Banner appropriate to article type will appear here in typeset article

Effects of surface roughness on the propulsive performance of pitching foils

Rodrigo Vilumbrales-Garcia^{1†}, Melike Kurt¹,
Gabriel D. Weymouth^{1,2}, and Bharathram Ganapathisubramani¹

¹Faculty of Engineering and Physical Sciences, University of Southampton, UK,

²Faculty of Mechanical, Maritime and Materials Engineering (3mE), TU Delft, NL

(Received xx; revised xx; accepted xx)

The hydrodynamic influence of surface texture on static surfaces ranges from large drag penalties (roughness) to potential performance benefits (*shark-like skin*). Although, it is of wide-ranging research interest, the impact of roughness on flapping systems has received limited attention. In this work, we explore the effect of roughness on unsteady performance of a harmonically pitching foil through experiments using foils with different surface roughness, at a fixed Strouhal number and within the Reynolds number (Re) range of $15k - 30k$. The foils' surface roughness is altered by changing the distribution of spherical-cap shaped elements over the propulsor area. We find that the addition of surface roughness does not improve the performance compared to a smooth surface over the Re range considered. The analysis of the flow fields shows near identical wakes regardless of the foil's surface roughness. The performance reduction mainly occurs due to an increase in profile drag. However, we find that the drag penalty due to roughness is reduced from 76% for a static foil to 16% for a flapping foil at the same mean angle of attack, with the strongest decrease measured at the highest Re . Our findings highlight that the effect of roughness on dynamic systems is very different than that on static systems, thereby, cannot be accounted for by only using information obtained from static cases. This also indicates that the performance of unsteady, flapping systems is more robust to the changes in surface roughness.

Key words: Flapping foils, surface roughness, propulsive performance

1. Introduction

Surface roughness is ever-present in engineering applications leveraging fluid-structure interactions. Its implications on the flow and the consequent drag generation have been widely studied in the related literature. From the influence of roughness in pipe flow (Achenbach 1971), to its effects on the trajectory of

† Email address for correspondence: r.vilumbrales-garcia@soton.ac.uk

a golf ball (Chowdhury *et al.* 2016), roughness plays a vital role in any application involving fluid-structure interaction considerations. For example, surface roughness can be detrimental to the performance of wind turbines. Sagol *et al.* (2013) found that the accumulation of contamination agents in the blades leads to a reduction in power extraction, while, Ehrmann *et al.* (2017) reported a performance decrease linked to an increase in roughness density and height. On the other hand, the use of roughness elements can lead to a drag reduction and certain performance gains for unsteady propulsion systems. Previous studies inspired from swimmers and flyers show that, from shark skin or dolphin skin (Dean & Bhushan 2010; Wainwright *et al.* 2019) to feathers on a wing of a gliding bird (Van Bokhorst *et al.* 2015), roughness in varying shapes and texture modifies the fluid flow over propulsor surfaces, leading to a reduction in drag or a decrease in flow separation. In engineering applications, Gad-el Hak & Bushnell (1991) analysed the effects of roughness turbulators and found a C_L/C_D increase when compared to a smooth foil for $Re \leq 100000$. Also, the use of surface riblets can lead to a decrease in skin friction when aligned in the flow direction (Bechert *et al.* 1997), achieving a drag reduction of up to 8% (Walsh 1982). When configured properly, surface roughness can be beneficial. It can reduce drag production and potentially improve the overall performance. Surface roughness can also have detrimental effects. Tailoring the surface roughness to have an improved performance requires a better understanding of the effect of shape, size, and area distribution of roughness elements on both the force production and the flow.

The drag-reduction potential of surface roughness on aquatic swimmers have been explored mainly for static surfaces. For example, sharks can reduce their skin friction when their riblets are aligned with the flow (Dean & Bhushan 2010). Bixler & Bhushan (2013) pointed out that the riblets lift and pin the vortices generated in the viscous sublayer, leading to a decrease in drag. Bechert *et al.* (2000) observed a drag reduction for interlocking 3D riblets. Afroz *et al.* (2016) concluded that 'shark-like' textures can act like a passive flow separation control mechanism. Du *et al.* (2022) found smaller separated regions and adverse pressure gradients for the flow over a foil covered with tilted biomimetic shark scales. The effect of the shape and size of the rough elements were analysed by Domel *et al.* (2018), highlighting the importance of the denticle shape, as they found a drag reduction only for the smaller of the three considered. Although surface roughness has shown promising potential for static bodies, its role in unsteady systems is still not clear. Shark-skin surfaces have been shown to increase the self-propelled swimming speed and reduce the drag of a flapping foil (Oeffner & Lauder 2012; Domel *et al.* 2018), but only when small denticles are used, whereas the larger elements can lead to an increase in drag. Wen *et al.* (2014) reported a reduction in energy consumption due to a formation of stronger leading-edge vortices. Guo *et al.* (2021) found that, for static foils towed at a constant velocity, the roughness elements resulted in a considerably thicker boundary layer when compared to the smooth foil, while, for static foils in acceleration, the changes due to roughness in the wake characteristics were considerably smaller. Mostly, previous work conclude that shark-inspired surfaces can improve the performance of an unsteady body, but the potential benefit is strongly dependent on the shape and size of shark denticles, which often appear in highly complex geometries. Therefore, it is still to be seen if such performance improvement can be achieved with simple, commercially available roughness elements, located on the surface of an unsteady foil in harmonic motions.

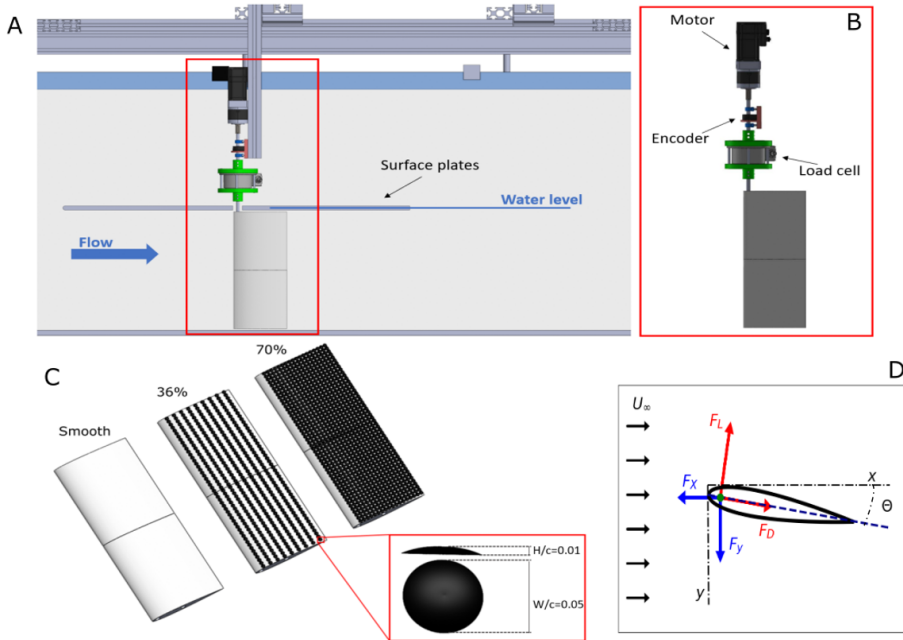


Figure 1: Schematics of the experimental setup in the water flume (A), the actuation arm (B), foils with three different roughness area coverage ratio (C), and the forces acting on the foil (D).

In this study, we analyse experimentally the effects of surface roughness on the propulsive performance of a pitching foil by using simple roughness elements. In Section 2, we define the methodology and experimental setup used to actuate three different foils with varying roughness characteristics. We investigate the effects of Reynolds number in the range of $15,000 \leq Re \leq 30,000$ and report the propulsive performance of a pitching aerofoil in terms of thrust production (C_X) and efficiency (η). In Section 3, we detail the force and flow measurement results obtained for flapping foils, and draw a comparison between dynamic and static foil cases.

2. Experimental setup and methodology

Force and flow measurements are conducted in a recirculating water flume at the University of Southampton, with a test section of 8.1 m length, 1.2m width and 0.9m depth. A surface plate is installed at the foil tip and the foil is placed right above the bottom wall to prevent tip vortex formation and enforce nominally two-dimensional flow over the foil as shown in Figure 1A.

Three foils with a rectangular planform and a NACA0012 cross-section were 3d-printed, with a chord-length of $c = 0.16m$ and an aspect ratio of $AR = 2.5$. Spherical-cap shaped roughness element with a width (diameter) of $W = 0.05c$ and height of $H = 0.01c$ (Dean & Bhushan 2010) were placed on pressure and suction sides of the foils. As shown in Figure 1C, in addition to the smooth foil, two different roughness levels are considered by varying the area occupied by the spherical-cap elements to 36% and 70% of the foil planform area.

Each foil was actuated with a stepper motor (Applied Motions STM23S) in sinusoidal pitching motions, about a point $0.08c$ distance from the leading edge.

Re	15,000	20,000	25,000	30,000
U [m/s]	0.10	0.14	0.17	0.21
f_0 [Hz]	0.62	0.83	1.03	1.24
St	0.25	0.25	0.25	0.25

Table 1: Experimental parameters used in the current study

The prescribed motion is defined by $\theta(t) = \theta_0 \sin(2\pi f_0 t)$, where θ_0 is the pitching amplitude and f_0 is the flapping frequency. The pitching amplitude θ_0 , Strouhal number $St = 2Af_0/U$, and reduced frequency $k = 2\pi f_0 c/U$ were fixed all throughout the experiments at $\theta_0 = 7.5^\circ$, $St = 0.25$ and $k = 6$, respectively, to ensure the foils to perform in the high-efficiency, thrust producing regime (Zurman-Nasution *et al.* 2021; Muscutt *et al.* 2017; Kurt & Moored 2018). A Reynolds number sweep ($Re = Uc/\nu$ where ν is the kinematic viscosity) was conducted within the range of $15,000 \leq Re \leq 30,000$ by varying the flow velocity. In this range, the propulsive performance was previously reported to be Re independent (Senturk & Smits 2019). A summary of the parameters used in this study is given in Table 1. The forces and moments acting on the foils were measured with a six-axis force sensor (ATI Gamma IP65). The motion was tracked using a rotary, incremental encoder (US Digital E5) attached on the motor shaft (Figure 1 B). Each trial was conducted for a total of 100 flapping cycles and repeated five times. The measured forces were filtered using a Butterworth filter with a low-pass frequency of five times the flapping frequency. The power was calculated as a multiplication of pitching moment and the angular velocity which was derived from the measured angular displacement. The instantaneous and time-averaged performance metrics are the average values from 500 flapping cycles, measured over five trials. To distinguish instantaneous forces from time-averaged results, the latter is denoted by $\overline{(\cdot)}$. The reported streamwise force (thrust) (C_X) and power (C_P) coefficients, and efficiency (η) are defined as,

$$C_X = \frac{F_X}{\frac{1}{2}\rho U^2 c}, \quad C_P = \frac{P}{\frac{1}{2}\rho U^3 c}, \quad \eta = \frac{C_X}{C_P} \quad (2.1)$$

where ρ is the density of water and U represents the free-stream flow velocity.

The force measurements were synchronised with planar Particle Image Velocimetry (PIV) measurements (cameras: *LaVision MX 4MP*, lasers: *Litron Nano PIV*). The field-of-view captures the entire foil and up to one chord-length in foil's wake. The software *Davis 10* was used to cross-correlate the acquired particle image pairs (with 24×24 pixels with 50% overlap). The flapping cycle was divided into twenty-two phases and twenty-five cycles were acquired per phase. The velocity fields corresponding to each phase was then averaged over 25 cycles.

3. Results

3.1. Flow-field and force production analysis of foils with different roughness area coverage ratios

Figure 2 compares the out-of-plane vorticity and the instantaneous performance coefficients, C_X and C_P for all the roughness cases considered at $Re = 25,000$. The first column (A,D), the second column (B,E) and the third column (C,F)

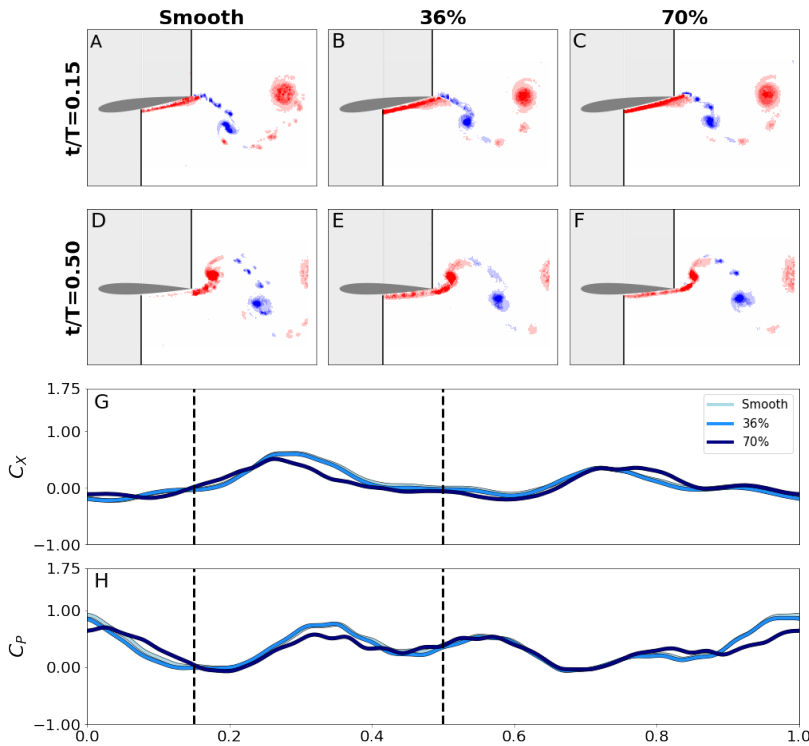


Figure 2: PIV results for $Re = 25000$. $t/T = 0.15$ (A,D,G) and $t/T = 0.50$ (B,E,H) for the Smooth (A,D), 36% (B,E) and 70% (C,F). Instantaneous C_X (H) and instantaneous C_P (I)

present the evolution of the vorticity field around three pitching foils with 0%, 36% and 70% surface roughness at $t/T = 0.15$, and $t/T = 0.50$, respectively. Surprisingly, change in the roughness does not lead to any significant alteration in the vorticity fields. Regardless of the roughness coverage, all foils produce a reverse von Karman-street where two counter-rotating vortices per flapping cycle are shed from the trailing edge into the wake, as widely observed in the related literature for smooth foils (Muscott *et al.* 2017; Kurt & Moored 2018; Zurman-Nasution *et al.* 2021). Figure 2 G-H presents the evolution of cycle-averaged thrust and power coefficients over one flapping cycle. Similar to the flow fields, the performance coefficients show only minor differences between the smooth foil and the foils with roughness. Although, we have only revealed the analysis associated with a single Re , these results hold across the Re range considered here. In the supplementary material, we present the evolution of the flow-field over one flapping cycle at $Re = 15,000$ and $Re = 25,000$ as videos for comparison. Overall, these results from force and flow field measurements show that incorporating surface roughness does not have a strong influence on the development of the wake. Other parameters, such as Strouhal number or kinematics (Schnipper *et al.* 2009) are known to significantly affect the evolution of the vortex structures, which can minimise the adverse effects on performance induced by the roughness elements.

Figure 3 introduces the spectral analysis conducted for C_X presented in Figure 2

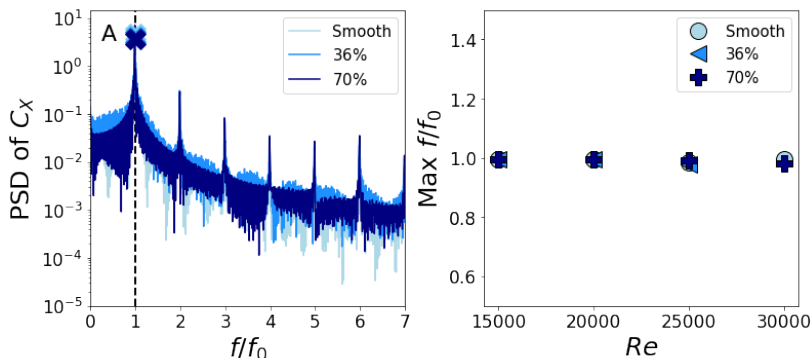


Figure 3: (A) Fast Fourier Transform (FFT) analysis of the instantaneous C_X at $Re = 25,000$. The cross indicates the location of the peak for each case. The vertical dashed bar denotes $f/f_0 = 1$. (B) Peak frequency across the Re values considered. A value of 1 denotes that the thrust force signal peak f is equal to the input pitching frequency f_0 .

G-H. The power spectra of the thrust force at $Re = 25,000$ is shown in (A). The crosses indicate the location of the peak frequency for each foil. In (B), we introduce the dominant frequency ratio in the form of f/f_0 , where f_0 is the prescribed pitching frequency across the Re range considered. This analysis shows that the dominant frequency in thrust production corresponds to the pitching frequency f_0 for all the Re values, and contains similar energy density for all the foils. This result combined with the similarities observed in both the wake and the instantaneous forces indicates that the performance of the foils is highly dominated by f_0 , hence, by the kinematics. The dominant effects of the frequency and the kinematics observed in our study are similar to the findings by Zurman-Nasution *et al.* (2021), who reported that compared to flapping frequency and kinematics, shape-related parameters such as sweep angle, have negligible effects on propulsive performance.

Figure 4 presents the change in cycle-averaged performance coefficients for foils with different roughness coverages against Re . Starting with $\overline{C_X}$ (Figure 4A), we compare our results with other NACA0012 studies conducted by Mackowski & Williamson (2015) ($Re = 16,600$, $0.1 \leq St \leq 0.4$), and Senturk & Smits (2019) ($500 \leq Re \leq 36,000$, $0.2 \leq St \leq 0.6$). Thrust, $\overline{C_X}$, obtained for the smooth foil increases slightly with Reynolds number, a trend similar to previous studies. The thrust values obtained at $St = 0.25$ in the current study fall within the findings by Senturk & Smits (2019) at $St = 0.2$ and $St = 0.4$. In the inset enclosed by a blue box, it is shown that C_X decreases with the addition of surface roughness across the Re range. In Figure 4B, our results indicate higher efficiency values than Mackowski & Williamson (2015) and Senturk & Smits (2019), which could be due to differences in the pivot point location (at $0.08c$ distance from the leading edge here, and at $0.25c$ distance in previous studies). For each roughness case, $\overline{C_P}$ slightly increases against Re , but regardless of the Re , increase in roughness causes a decrease in $\overline{C_P}$. The efficiency also decreases as the surface roughness increases, similar to thrust and power. Although the flow fields show negligible alterations with the change in roughness, the cycle averaged forces point to a performance reduction as the roughness increases. The thrust decrease observed for 36% and 70% roughness coverages compared to smooth foil can be related to an increase in the profile drag. To further explore this effect, in the next figure,

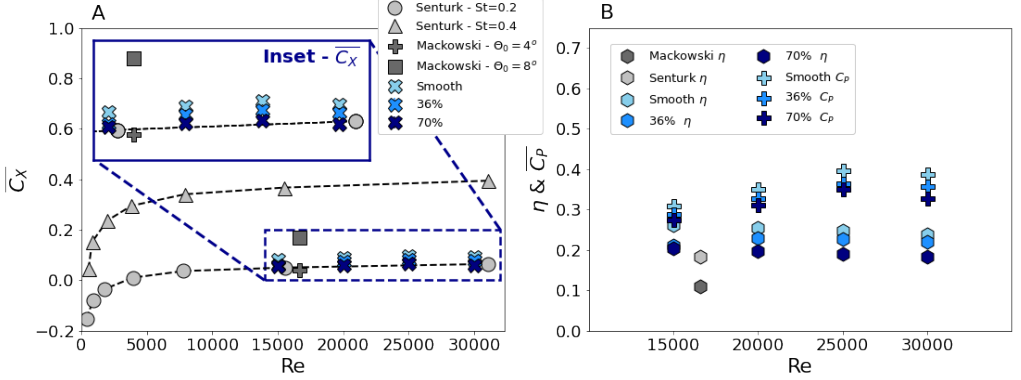


Figure 4: A) \overline{C}_X obtained in the current study (blue range) and compared with previous studies against Re : Senturk & Smits (2019) (gray) and Mackowski & Williamson (2015) (dark-gray). The data enclosed by the blue box presents an inset of \overline{C}_X data for the Re range of $15,000 \leq Re \leq 30,000$. B) \overline{C}_P results (hexagon) and η (cross) for current and previous studies, marked by the same colours used in A.

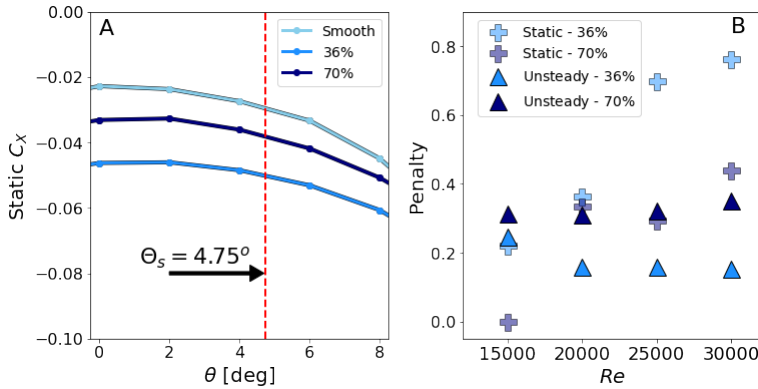


Figure 5: A) static C_X vs angle of attack θ measured using static foils at $Re = 25,000$. Smooth foil presented in light-blue, 36% in medium-blue, and 70% in dark-blue. The red dashed-line indicates the θ used to compare with the unsteady regime, defined as $\theta_s = 4.75^\circ$. B) Thrust and drag penalty due to roughness for both the flapping (triangles) and static results (crosses) for the 36% case (medium blue) and the 70% case (dark blue).}

we have compared our flapping foil results with static foil measurements carried out using the same foils within the same Re range.

3.2. Comparison between static and flapping regimes

In this section, we introduce the data collected for static foils and compare it with the pitching foil results to further explore why there is a change in thrust production with a change in roughness coverage. The static data was acquired within the same Re range and roughness coverages as the flapping cases, for an angle of attack (θ) range of $-4^\circ \leq \theta \leq 20^\circ$. To compare both scenarios, we have selected an angle of attack value equal to the average θ experienced by the foil during half the pitching cycle (red dashed-line in Figure 5A, denoted as θ_s). Next, we develop a comparison parameter or *penalty*, that evaluates the change in streamwise force generated by the smooth and rough foils. Given that static

state will produce drag (for all three foils) and the flapping cases produce thrust, we present the penalty in its absolute value to help with the comparison. Since we have found surface roughness to be detrimental for $\overline{C_X}$ for all cases considered, a positive penalty value in the static state indicates an increase in drag due to roughness elements, while $Penalty > 0$ in the flapping regime means a decrease in thrust caused by the roughness elements. Here, $Penalty$ is defined as the relative change in thrust for a rough foil compared to the smooth, $|(C_{X,rough} - C_{X,smooth})|/C_{X,smooth}$.

The penalty parameter is presented in Figure 5 for static foil (crosses) and flapping foil measurements (triangles). The addition of surface roughness increases the drag production in the static state across the Re range considered. At $Re = 30,000$, it reaches a 76% drag penalty for the 36% roughness and 43% penalty for the 70% roughness coverage, compared to the smooth foil. On the other hand, the flapping foils with roughness generate less thrust across the Re range compared to the smooth foil. At $Re = 30,000$, the thrust decreases by 35% and 16% for 70% and 36% roughness coverages, respectively. However, the flapping state appears to be more robust to Re changes. It reduces the penalty observed for static foils, especially for the 36% coverage. At $Re = 30,000$, foils with 36% coverage experiences a roughness penalty of 76% in the static state compared to a 16% penalty in the flapping state, which could be explained by the dominant effect that St and the kinematics have on force production.

To further analyse the data presented in Figure 5, we present the out-of-plane vorticity (ω_z) in Figure 6. The first row consists of the cycle-averaged unsteady pitching ω_z , and the positive vorticity regions are enclosed with isolines. In second and third rows, we present the flow-field data measured at $\alpha = 6^\circ$ for a pitching foil and a static foil, respectively. The first three columns correspond to 0% (smooth), 36% and 70% roughness coverages, respectively. The fourth column introduces a comparison between different roughness cases with overlapped ω_z isolines. The comparison of all three flapping cases suggests that the addition of surface roughness does not introduce major changes in shedding shear layers. In contrast, in the static state, foils with 36% and 70% roughness have thicker shear layer in time-average compared to the smooth case, similar to the findings by Guo *et al.* (2021). The presence of thicker shear layers for the roughness cases can be the culprit of 76% drag penalty shown in Figure 5.

4. Conclusions

In this study, we have analysed the influence of surface roughness on the propulsive performance of flapping foils, using force and flow measurements. Three NACA0012 foils with different roughness coverage ratios have been constructed, and tested within the Reynolds number range of $15,000 \leq Re \leq 30,000$. We have found that the addition of surface roughness is detrimental to thrust production and efficiency of a pitching foil. The foils with 36% and 70% roughness produce 16% and 35% less thrust, respectively, compared to the smooth foil. We have determined that Re does not play an important role on neither the thrust nor efficiency for the Re range and roughness coverage ratios considered. Although we have seen no significant change in the wake flow, the foils with roughness experience a decrease in thrust and efficiency, which can be explained by an increase in profile drag associated with the roughness elements. We have compared the effects of roughness on static and flapping states, finding

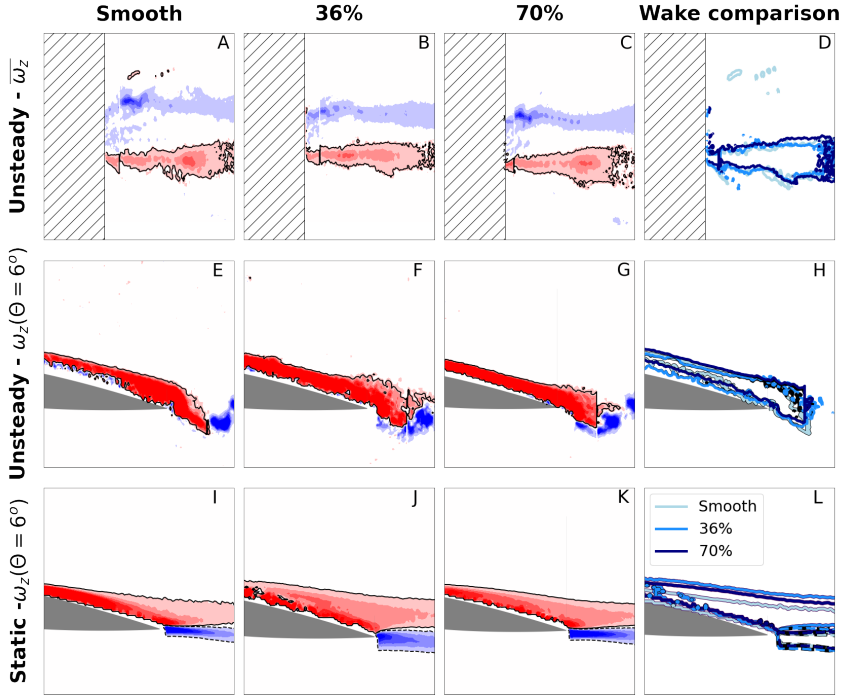


Figure 6: Pitching cycle-averaged vorticity (A,B,C), flapping instantaneous vorticity at $\theta = 6^\circ$ degrees (E,F,G) and static PIV results at $\theta = 6^\circ$ (I,J,K). Smooth foil (A,E,I), 36% (B,F,J), and 70% (C,G,K). The comparison of the wakes generated by the foils at each of the conditions is presented at (D,H,L)

that the former is considerably more sensitive to it. The roughness penalty for 36% roughness coverage is reduced from 76% in the static state to 16% for flapping. The strongest decrease occurs at the highest Re, highlighting that the effect of roughness on flapping systems is very different than on static systems. This shows that the performance of flapping systems is more robust to the changes in surface roughness.

Declaration of Interests: The authors report no conflict of interest.

Acknowledgements

This research was supported financially by the Office of Naval Research Global Award N62909-18-1-2091, the Engineering and Physical Sciences Research Council (Grant No: EP/R034370/1) and the doctoral training award.

Data availability statement

All data supporting this study will be made openly available from the University of Southampton repository upon publication.

REFERENCES

- ACHENBACH, ELMAR 1971 Influence of surface roughness on the cross-flow around a circular cylinder. *Journal of fluid mechanics* **46** (2), 321–335.
- AFROZ, FARHANA, LANG, AMY, HABEGGER, MARIA LAURA, MOTTA, PHILIP & HUETER,

- ROBERT 2016 Experimental study of laminar and turbulent boundary layer separation control of shark skin. *Bioinspiration & biomimetics* **12** (1), 016009.
- BECHERT, DW, BRUSE, M & HAGE, W 2000 Experiments with three-dimensional riblets as an idealized model of shark skin. *Experiments in fluids* **28** (5), 403–412.
- BECHERT, DW, BRUSE, M, HAGE, W VD, VAN DER HOEVEN, JG TH & HOPPE, G 1997 Experiments on drag-reducing surfaces and their optimization with an adjustable geometry. *Journal of fluid mechanics* **338**, 59–87.
- BIXLER, GREGORY D & BHUSHAN, BHARAT 2013 Fluid drag reduction with shark-skin riblet inspired microstructured surfaces. *Advanced Functional Materials* **23** (36), 4507–4528.
- CHOWDHURY, HARUN, LOGANATHAN, BAVIN, WANG, YUJIE, MUSTARY, ISRAT & ALAM, FIROZ 2016 A study of dimple characteristics on golf ball drag. *Procedia engineering* **147**, 87–91.
- DEAN, BRIAN & BHUSHAN, BHARAT 2010 Shark-skin surfaces for fluid-drag reduction in turbulent flow: a review. *Philosophical Transactions of the Royal Society A: Mathematical, Physical and Engineering Sciences* **368** (1929), 4775–4806.
- DOMEL, AUGUST G, DOMEL, GINO, WEAVER, JAMES C, SAADAT, MEHDI, BERTOLDI, KATIA & LAUDER, GEORGE V 2018 Hydrodynamic properties of biomimetic shark skin: effect of denticle size and swimming speed. *Bioinspiration & biomimetics* **13** (5), 056014.
- DU, ZENGZHI, LI, HONGYUAN, CAO, YUFAN, WAN, XIA, XIANG, YAOLEI, LV, PENGYU & DUAN, HUILING 2022 Control of flow separation using biomimetic shark scales with fixed tilt angles. *Experiments in Fluids* **63** (10), 1–12.
- EHRMANN, ROBERT S, WILCOX, BENJAMIN, WHITE, EDWARD B & MANIACI, DAVID CHARLES 2017 Effect of surface roughness on wind turbine performance. *Tech. Rep.*. Sandia National Lab.(SNL-NM), Albuquerque, NM (United States).
- GUO, PENGMING, ZHANG, KAI, YASUDA, YUJI, YANG, WENCHAO, GALIPON, JOSEPHINE & RIVAL, DAVID E 2021 On the influence of biomimetic shark skin in dynamic flow separation. *Bioinspiration & Biomimetics* **16** (3), 034001.
- GAD-EL HAK, MOHAMED & BUSHNELL, DENNIS M 1991 Separation control .
- KURT, MELIKE & MOORED, KEITH W 2018 Flow interactions of two-and three-dimensional networked bio-inspired control elements in an in-line arrangement. *Bioinspiration & biomimetics* **13** (4), 045002.
- MACKOWSKI, AW & WILLIAMSON, CHK 2015 Direct measurement of thrust and efficiency of an airfoil undergoing pure pitching. *Journal of Fluid Mechanics* **765**, 524–543.
- MUSCUTT, LE, WEYMOUTH, GD & GANAPATHISUBRAMANI, BHARATHRAM 2017 Performance augmentation mechanism of in-line tandem flapping foils. *Journal of Fluid Mechanics* **827**, 484–505.
- OEFFNER, JOHANNES & LAUDER, GEORGE V 2012 The hydrodynamic function of shark skin and two biomimetic applications. *Journal of Experimental Biology* **215** (5), 785–795.
- SAGOL, ECE, REGGIO, MARCELO & ILINCA, ADRIAN 2013 Issues concerning roughness on wind turbine blades. *Renewable and sustainable energy Reviews* **23**, 514–525.
- SCHNIPPER, TEIS, ANDERSEN, ANDERS & BOHR, TOMAS 2009 Vortex wakes of a flapping foil. *Journal of Fluid Mechanics* **633**, 411–423.
- SENTURK, UTKU & SMITS, ALEXANDER J 2019 Reynolds number scaling of the propulsive performance of a pitching airfoil. *Aiaa Journal* **57** (7), 2663–2669.
- VAN BOKHORST, EVELIEN, DE KAT, ROELAND, ELSINGA, GERRIT E & LENTINK, DAVID 2015 Feather roughness reduces flow separation during low reynolds number glides of swifts. *Journal of Experimental Biology* **218** (20), 3179–3191.
- WAINWRIGHT, DYLAN K, FISH, FRANK E, INGERSOLL, SAM, WILLIAMS, TERRIE M, ST LEGER, JUDY, SMITS, ALEXANDER J & LAUDER, GEORGE V 2019 How smooth is a dolphin? the ridged skin of odontocetes. *Biology letters* **15** (7), 20190103.
- WALSH, M 1982 Turbulent boundary layer drag reduction using riblets. In *20th aerospace sciences meeting*, p. 169.
- WEN, LI, WEAVER, JAMES C & LAUDER, GEORGE V 2014 Biomimetic shark skin: design, fabrication and hydrodynamic function. *Journal of Experimental Biology* **217** (10), 1656–1666.
- ZURMAN-NASUTION, ANDHINI N, GANAPATHISUBRAMANI, BHARATHRAM & WEYMOUTH, GABRIEL D 2021 Fin sweep angle does not determine flapping propulsive performance. *Journal of the Royal Society Interface* **18** (178), 20210174.